Vol. 23, No. 3(2024) IE24252
Revista Mexicana de Ingeniería Química

Preformed oil-in-water macroemulsions for oil recovery

Macroemulsiones preformadas de tipo aceite en agua para la recuperación de petróleo

O. Olivares-Xometl[1], P. Arellanes-Lozada[4], I. V. Lijanova[2], L. Azotla-Cruz[3], N. V. Likhanova[4]*
[1] *Benemérita Universidad Autónoma de Puebla, Av. San Claudio y 18 Sur, C.P. 72570, Ciudad Universitaria, Puebla, Puebla, México.*
[2] *Centro de Investigación e Innovación Tecnológica del Instituto Politécnico Nacional, Cerrada de CECATI S/N, Col. Santa Catarina, C.P. 02250, CDMX, México.*
[3] *Centro de Tecnologías para Exploración y Producción del Instituto Mexicano del Petróleo, Camino de Terracería # 800, C.P. 94286, Col. San José Novillero, Boca del Río, Veracruz, México.*
[4] *Direccion de Investigación, Instituto Mexicano del Petróleo, Eje Central Lázaro Cárdenas No. 152, Col. San Bartolo Atepehuacan, C.P. 07730, CDMX, México.*
Received: December 24, 2023; Accepted: May 20, 2024

Abstract
Laboratory experiments were run by injecting 0.1 pore volume of emulsion slug of diluted oil-in-water emulsion at 1 wt. % of the dispersed oil phase through sandstone cores, imitating "single well" and "two well" injection. Oil displacement tests were carried out as part of a secondary recovery process, followed by the injection of an emulsion slug, and then again by water flooding to obtain additional oil recovery: 19 – 23 % for the "single well" test and up to 33 % for the "two-well" test, which was monitored through X-ray diffraction. A series of emulsion preparation tests was carried out to identify the best emulsifier, stirring time and rate, finally achieving an emulsion with average size of the dispersed droplets of 0.9 μm. The recovery percentage by emulsion injection is due to a soft blocking effect of the pore throats, where the emulsion is trapped, which changes the pattern of the preferential channels of water; as a consequence, water reaches areas that were not previously penetrated during the waterflooding operation as secondary recovery technique.
Keywords: oil-in-water emulsion, additional oil recovery, macroemulsion, Berea sandstone, tomography.

Resumen
Los experimentos de laboratorio se realizaron inyectando un lote de emulsión, al 1% en peso de la fase aceitosa dispersa y equivalente a 0.1 del volumen poroso, a través de núcleos de roca arenisca imitando inyección en "un pozo" y "dos pozos". Las pruebas de desplazamiento de petróleo se llevaron a cabo como parte de un proceso de recuperación secundaria, seguidas de la inyección de un lote de emulsión, obteniendo una recuperación adicional de petróleo: 19 – 23 % para la prueba de "un pozo" y hasta 33 % para la prueba de "dos pozos", que se monitoreó mediante tomografía. Se llevaron a cabo una serie de pruebas de preparación de la emulsión para identificar el mejor emulgente, tiempo de agitación y velocidad, logrando finalmente una emulsión con un tamaño promedio de las gotas dispersadas de 0.9 μm. El porcentaje de recuperación por inyección de emulsión se debe a un suave efecto de bloqueo de las gargantas de los poros, donde queda atrapada la emulsión, lo que cambia el patrón de los canales preferenciales de agua; como consecuencia, el agua llega a las áreas que no fueron previamente barridas durante la recuperación secundaria por inyección de agua.
Palabras clave: emulsión tipo aceite en agua, recuperación adicional de petróleo, macroemulsión, arenisca Berea, tomografía.

* *Corresponding author. E-mail*: nvictoro@imp.com.mx;
https://doi.org/10.24275/rmiq/IE24252
ISSN:1665-2738, *issn-e*: 2395-8472

1 Introduction

Dispersed suspensions or emulsion-type systems are injected into oil reservoirs to block rock pores and reduce the permeability and sometimes change the rock wettability, which entails the alteration of the water flow direction, and improvement of the sweep efficiency of injected water.

The formation process of emulsions within a reservoir occurs during the alkali/surfactant/ polymer flooding, when alkalis and surfactants emulsify crude oil by decreasing the interfacial tension between the hydrocarbon phase and water (Schramm, 2006; Zabar *et al*., 2023; Z. Zhang *et al*., 2023). For this purpose, *in-situ*-prepared emulsions are commonly used through the injection of a surfactant micellar solution to emulsify oil and mobilize it through the porous medium (Castillo-Campos *et al*., 2021; Du *et al*., 2023; Goswami *et al*., 2018; X. Wang *et al*., 2022). The use of micellar flooding with surfactant for high salinity (198,000 mg/L) and high-temperature conditions (90 °C) requires high surfactant concentrations (oleic acid imidazoline) no less than 10 % (Ge *et al*., 2020).

The mechanism (and as a consequence, the amount of recovered hydrocarbon) varies depending on the presence of a micro- or macroemulsion. The blocking effect of the pores in the most permeable channels is the main mechanism of macroemulsions. Furthermore, this type of emulsions behaves differently depending on the capillary number (Nc) and this behavior pattern exerts a direct effect on the amount of recovered oil, e.g. in experiments with Nc = 2×10^{-5}, a maximum of 55 % of oil was recovered, whereas in experiments with Nc = 2×10^{-4}, a maximum of 20 % of additional oil was obtained (Guillen *et al*., 2012; Moradi *et al*., 2014; Ponce F. *et al*., 2017). Macroemulsions block the rock pores to control mobility and this plugging is governed by the resistance that a substance opposes to flow through a capillary system, i.e. by the *Jamin* effect (Ding *et al*., 2019; Z. Liu *et al*., 2019). In a nucleus with highly permeable channels, 617 μm width, when an emulsion flows through it, the apparent emulsion viscosity grows because all the drops push each other at random. In contrast, in a permeability porous medium with fracture widths from 27 to 67 μm, the emulsion drops get aligned within the narrow channels and then, the emulsion viscosity diminishes (Xu *et al*., 2017).

Microemulsions and nanoemulsions possess mechanism types that are different to the already reviewed one of macroemulsions for additional oil recovery. Due to the small size (below 0.5μm), the disperse phase particles flow through the porous medium without provoking blocking, reducing the interfacial tension (N. Kumar *et al*., 2021; Santanna *et al*., 2013), and causing the system to behave as if it consisted of a single phase, thus achieving mobility and diminishing the oil viscosity. In addition, the oil displacement is directly proportional to the viscosity increase of the employed microemulsion (de Castro Dantas *et al*., 2017). In this context, the development of Pickering or nanoparticle-stabilized emulsions for enhanced oil recovery (EOR) purposes has advanced in the last decade (Hou & Sheng, 2023; Jiang *et al*., 2023; Z. Wang *et al*., 2021) due to their thermal stability and suitable viscosity (ShamsiJazeyi *et al*., 2014). The silica (G. Kumar *et al*., 2023; Lu & Wang, 2023), metallic or aluminosilicate clay (halloysite) S (Sharma, Velmurugan, *et al*., 2015; L. Zhang *et al*., 2019), organoclay (Cloisite 15A) (Mohamed *et al*., 2018), polymer-Ag nanocomposite (Narukulla *et al*., 2020), or hydrophobic nanoparticles have been employed to stabilize Pickering emulsions and provide thermal stability (Jalilian *et al*., 2019; Sharma, Kumar, *et al*., 2015). But the use of nanoparticle-stabilized emulsions at reservoir level is doubtful due to the likely high cost of these composites and nanoparticles (Yoon *et al*., 2016).

Scientific interest has emerged in the last decade in the application of macroemulsions for EOR processes, e.g. in countries like United States, China and Brazil, where both oil recovery by water injection (including seawater) and enhanced recovery are common practices. The injection of emulsions can be employed to mitigate gravity segregation or what has been referred to as "water tongue" in a porous medium, thus producing uniform water sweeping (Baldygin *et al*., 2014; de Farias *et al*., 2012). The injection of 1.5 - porous volume (PV) of preformed macroemulsion with dispersed phase of a 22° API gravity Brazilian crude and the surfactant Steol CS-330 produces 69.9 % oil recovery. In this experiment, three aspects were identified: 1) the blocking of pores reduces irreversibly the permeability; 2) the injection of emulsions lowers the water-oil ratio with respect to a water-injection process; and 3) the effect exerted by the diameter of the disperse phase in the flow is a function of the capillary number when the drops are bigger than the diameter of pores through which emulsion drops should flow (de Farias et al., 2012). There is a relationship between the drop size in some crude-oil-based macroemulsions, pore throat radio, rock pore radio and additional oil recovery (Zhou *et al*., 2018, 2019).

Under oil-wet conditions, there is partially continuous pore wall transportation of the oil phase, while in a water-wet medium, the oil phase along the pore forms incomplete bridges and bypassed oil saturation (Yadali Jamaloei & Kharrat, 2010). There are emulsions that when injected into the reservoir, modify the rock wettability (Demikhova *et al*., 2014, 2016; Engelke *et al*., 2013). One of the best emulsion

performances, based on rock hydrophilization, was shown by polysiloxane-based systems tested at a Hungarian gas field (Lakatos *et al*., 2002, 2003, 2008).

The most common emulsions are prepared based on some oil fractions or heavy oil (Ding *et al*., 2019; J. Liu *et al*., 2023; O. Olivares-Xometl *et al*., 2021). Jatropha oil and diesel emulsions have been used for matrix-acidizing purposes (Yousufi *et al*., 2019). The discontinuous hydrocarbon phase, based on hydrocarbons such as diesel oil, naphtha, crude oil, with concentration was up to 10 wt.%, while the concentration of surfactants was up to 5 wt.%, reaching additional oil recovery up to 19 wt.% using 0.20 pore volumes of emulsion in Berea cores with temperatures and salinities up to 115 °C and 164,000 ppm, respectively (Cardenas *et al*., 1981; Shupe & Jr, 1981). Later, Karambeigi, found that the most important critical factors were salinity and surfactant concentration (Karambeigi *et al*., 2015).

Preformed emulsions are advantageous when being designed, because it is possible to have higher control of the particle size, which is directly related to two important aspects: emulsion stability and type of action mechanism in a porous medium (Hernandez-Perez *et al*., 2022). Based on the foregoing, the present work deals with the effect of a preformed O/W emulsion consisting of 1 wt.% of the dispersed oil phase and 0.04 wt.% of surfactant concentration on the additional oil recovery process in a sandstone rock medium by injecting 10 % of the total PV in a nucleus at 80 °C with injected water salinity of 100,000 ppm.

2 Experimental part

2.1 Emulsion preparation and characterization

An O/W emulsion was prepared by direct emulsification of 70 g of a hydrophobic compound with empirical formula $C_{18}H_{34}O_2$ (Sigma-Aldrich, technical grade 90 %, density@25 °C of 890 kg/m^3, n20/D of 1.459, and melting point of 13-14 °C) in 30 g of the aqueous phase, mixing with an Ultra-Turrax T25 Basic homogenizer from IKA at 16000 rpm for 8 min. The aqueous phase consisted of 3 g of Igepal CO 890 (Sigma-Aldrich, hydrophilic surfactant with HLB 17), 0.2 g of polyvinylpyrrolidone (Sigma-Aldrich) and 26.8 g of distilled water. The used emulsion was of the O/W type and the D_{90}, D_{50}, D_{10} were equal to 1.10, 0.70, and 0.59 μm, respectively. The diameter sizes were measured by using a laser diffraction piece of equipment Mastersizer 2000 Hydro2000S by Malvern, and Single Particle Optical Sensing (SPOS)/Light Obscuration (LO) by using a single particle optical sizer model Accusizer 780, calibrated and verified with Duke Scientific certified standards with traceability to NIST. The system employed for measuring the Z potential was a NanoBrook ZetaPlus piece of equipment by Brookhaven Instruments, using the electrophoretic light scattering (ELS) technique.

As for the Sauter mean diameter (D_{32}), it is defined as a hypothetical diameter equivalent to a uniform arrangement of drops with the same total volume and same surface area of the drops contained in the real liquid total volume, it is expressed quantitatively according to Equation (1):

$$D_{32} = \frac{\sum_i N_i D_i^3}{\sum_i N_i D_i^2} \tag{1}$$

where D_i is the diameter of each drop and N_i is the number of drops with diameter D_i. The prepared emulsion was diluted with distilled water before being used until obtaining 1 wt. % of the dispersed oil phase; the viscosity and density of the diluted emulsion were equal to those of water (1 cP and 1 g/mL, respectively).

2.2 Oil and brine

Crude oil used to prepare the crude blend type for export remarketing was acquired from a mature Mexican oil field (API gravity@20°C equal to 20.1 °API). Brine (NaCl salinity was 266881 ppm, total water hardness ($CaCO_3$ and $MgCO_3$) was 63300 ppm, Fe^{2+} concentration was 0.41 ppm, density@20 °C was 1176.4 kg/m^3, pH value of 5.95 and Stiff & Davis Stability index equal to 1.62191) from the same Mexican oil field was diluted with distilled water (until 100,000 ppm of NaCl) and used as displacement fluid.

2.3 Emulsion flooding in Berea cores

Berea Sandstone^{TM} (Cleveland Quarries) cores, coming from the same block, were used as porous media, and characteristics such as porosity (ϕ_0), water permeability (k_0), length (L) and diameter (D) are shown in Table 2. The experimental setup (Figure 1) consisted of an injection system with four positive displacement pumps, fluid sample bottles, a Berea sandstone cylinder, placed horizontally in a 2”- diameter and 4”-long core holder, a hand hydraulic pump for confining pressure, a back pressure regulator, and a differential pressure transducer. The displacement tests were carried out at constant confinement pressure of 13.79 MPa and 80 °C. The outline was: 1) after measuring the permeability of every previously cleaned and dried sandstone core, full saturation with brine proceeded by injecting it at a constant inlet flow rate of 10 cm^3/h for 24 h; 2) brine was drained through crude oil injection until reaching the residual connate water saturation (S_{wr}) (primary drainage); 3) oil was displaced at least by 5 PVs of brine injection at a constant inlet flow rate of 10 cm^3/h until reaching the residual oil saturation (S_{or}) (secondary recovery) and the produced fluids

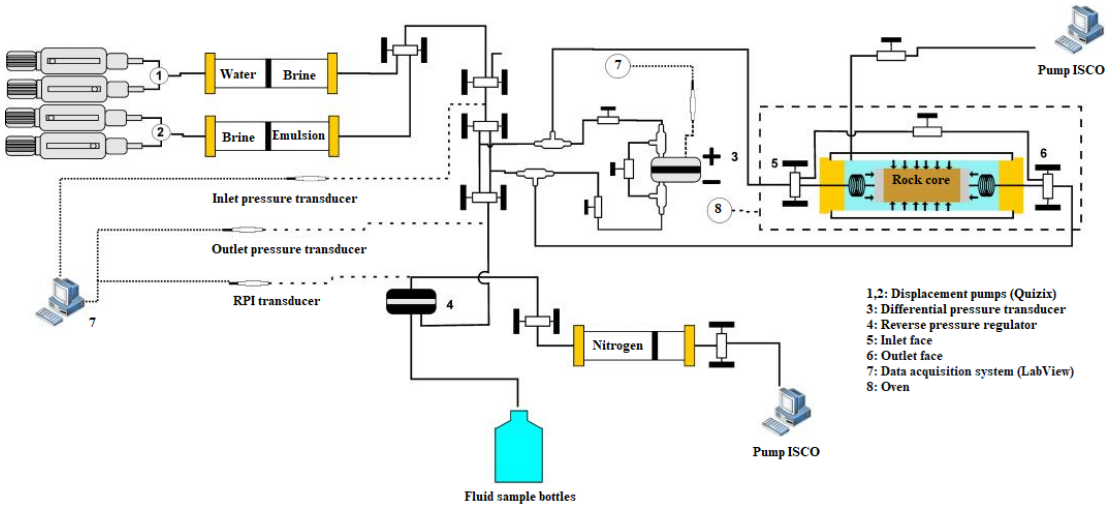

Figure 1. Experimental setup of an injection system.

a) b)

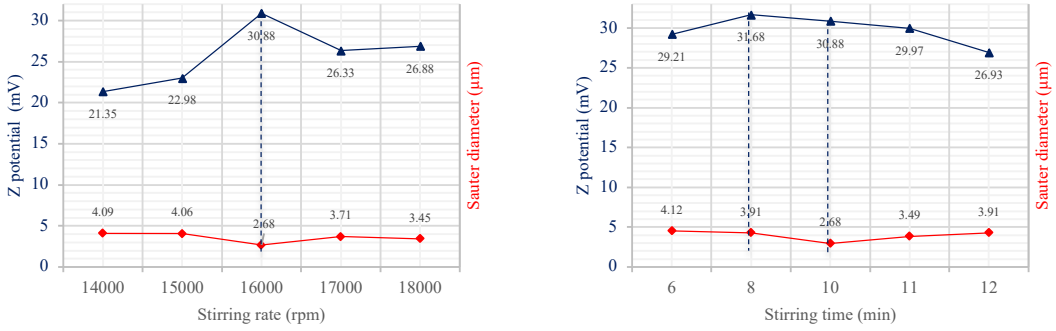

Figure 2. Behavior of Igepal CO 890: a) stirring rate vs Z potential values; b) stirring time vs Z potential values.

were collected and measured; 4) a slug of 0.1 PV, with an emulsion concentration of 1.0 wt.%, was injected from the outlet face of fluids opposite to the brine flow, followed by additional brine injection at a constant inlet flow rate of 10 cm^3/h through the inlet face opposite to the emulsion flow (tertiary recovery). The produced fluids were collected and measured.

2.4 Tomography study of the displacement test in the rock nuclei

The displacement test was carried out in a system coupled to an X-ray tomography scanner Philips Brilliance that allows imaging with spacing of 3 mm. The displacement tests were carried out at confinement pressure of 6.90 MPa and 80 °C. The outline was: 1) after measuring the permeability of every previously cleaned and dried sandstone core, full saturation with brine occurred by injecting it at a constant inlet flow rate of 10 cm^3/h for 24 h; 2) brine was drained by means of crude oil injection until reaching the residual connate water saturation (S_{wr}) (primary drainage); 3) oil was displaced at least by 5 PVs of brine injection at a constant inlet flow rate of 5 cm^3/h until reaching the residual oil saturation and the produced fluids were collected and measured; 4) a slug of 0.1 PV, with an emulsion concentration of 1.0 wt.%, was injected from the inlet face of fluids, followed by additional brine injection at a constant inlet flow rate of 10 cm^3/h through the inlet face of fluids (tertiary recovery) until the oil production came to a stop. The produced fluids were collected and measured.

3 Results and discussion

3.1 Preformed oil-in-water emulsion

The kinetic stability of the O/W emulsions is a consequence of the small size of the drops

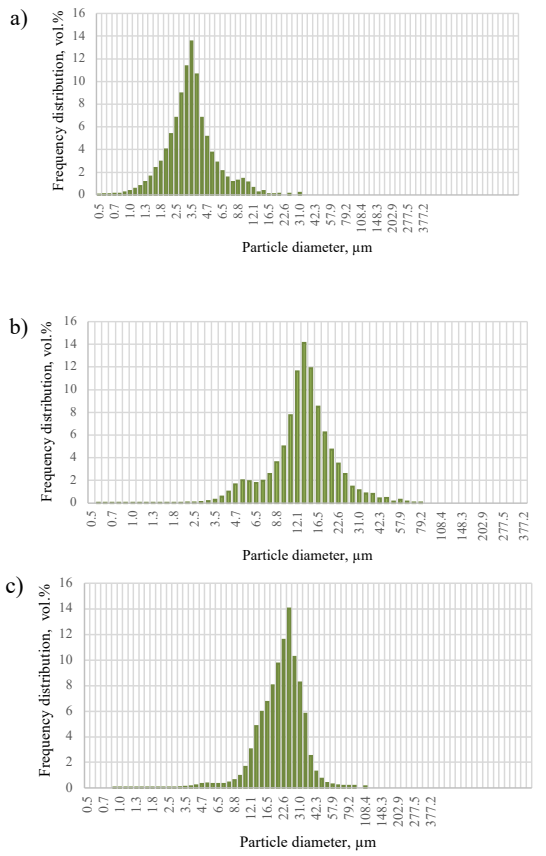

Figure 3. Distribution of the drop size in the emulsions with 2 wt.% of: a) Igepal CO 890; b) Tergitol NP-40; and c) Brij L23.

and presence of an interfacial film around the oil drops. To form O/W emulsions, emulsifiers with hydrophilic-lipophilic balance (HLB) between 10 and 18 are employed. To this end, three emulsifiers were screened: Tergitol NP-40, Igepal CO 890 and Brij L23 with HLB values of 17.8, 17.0 and 16.9, respectively. Tergitol NP-40 and Igepal CO 890 are non-ionic emulsifiers based on low-molecular-weight polymers derived from nonylphenol ethoxylate and have an aromatic ring and repeated polyethoxyl group, whereas Brij L23 consists of polyoxyethylene lauryl ether. The composition of the emulsions always kept 70 wt.% of the oily phase with the surfactant concentration of 2 wt.%; the water content corresponded to the one necessary to complete 100 %. The adequate dispersion rate was established, preparing the Igepal CO 890-based emulsions by varying the revolutions per minute (rpm) between 14000 and 18000; furthermore, the dispersion time was analyzed and then, preparations were carried out at times equal to 6, 8, 10, 11 and 12 min and 16000 rpm (Figure 2). The most suitable parameters were stirring rate of 16000 rpm and stirring times from 8 to 10 min. For this reason, all the emulsions with concentration of the corresponding emulsifier of 2 wt.% were prepared under these conditions.

Table 1. Z potential and mean Sauter diameter data of the emulsions with different emulsifiers at concentration of 2 wt.%.

Emulsifier	Z potential (mV)	D_{32} (μm)
Igepal CO 890	30.88	2.68
Tergitol NP-40	26.91	11.96
Brij L23	31.6	20.54

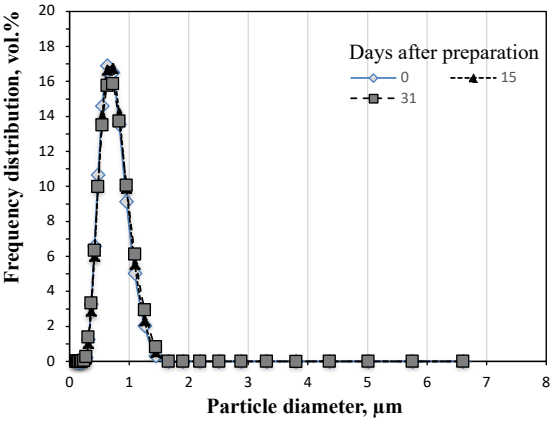

Figure 4. Drop size distribution plots of the emulsion with 3 wt.% of Igepal CO 890 measured by using laser diffraction.

Tergitol NP-40 and Igepal CO 890, due to the fact that the aromatic ring favors stronger interactions with the unsaturated chain of the compound representing the emulsion oily phase, presented better performance forming emulsions with the disperse phase particles with lower sizes (2.68-11.96 μm), which is in contrast with the Brij L23-based emulsion (20.54 μm); in addition, the size distribution of the emulsion particles, measured by SPOS/LO, presented monomodal behavior (Figure 3). In this case, the Sauter diameter (D_{32}) indicates that the emulsion drops presented a low trend to coalesce, which is closely related to the stability of emulsions.

In general, particles dispersed in a liquid have a charge on their surface and when an electric field is applied, the particles in the disperse phase flow at a velocity that is proportional to the charge magnitude and for this reason, the Z potential can be calculated. It was observed that the three emulsions displayed appropriate stability, for their absolute Z potential values were close to 30 mV (Table 1).

Finally, it was decided to prepare an emulsion at stirring rate of 16000 rpm, with stirring time of 8 min and Igepal CO 890 as emulsifier, increasing its concentration up to 3 wt.% and adding 0.2 wt.% of polyvinylpyrrolidone as stabilizer; the concentration of the oily phase was preserved at 70 %. The formed emulsion had D_{32} size of 0.9 μm and Z potential equal to 36.3 mV, being stable for 30 days without exhibiting the coalescence phenomenon (Figure 4); for

Table 2. Properties of Berea cores and oil recovery results.

Core	L [m]	D [m]	k_0 [mD]	φ_0 [%]	Initial oil saturation [%]	Cumulative oil recovery [%]			
						Water flooding, R_w	Emulsion flooding, R_e	Total	Residual oil recovery, R_r
1	0.099	0.0508	11.58	16.64	85.26	49.71	9.55	59.26	19
2	0.098	0.0508	32.77	20.08	88.7	43.8	10.66	54.46	19
3	0.098	0.0508	45.91	18.34	78.25	41.68	13.35	55.03	23

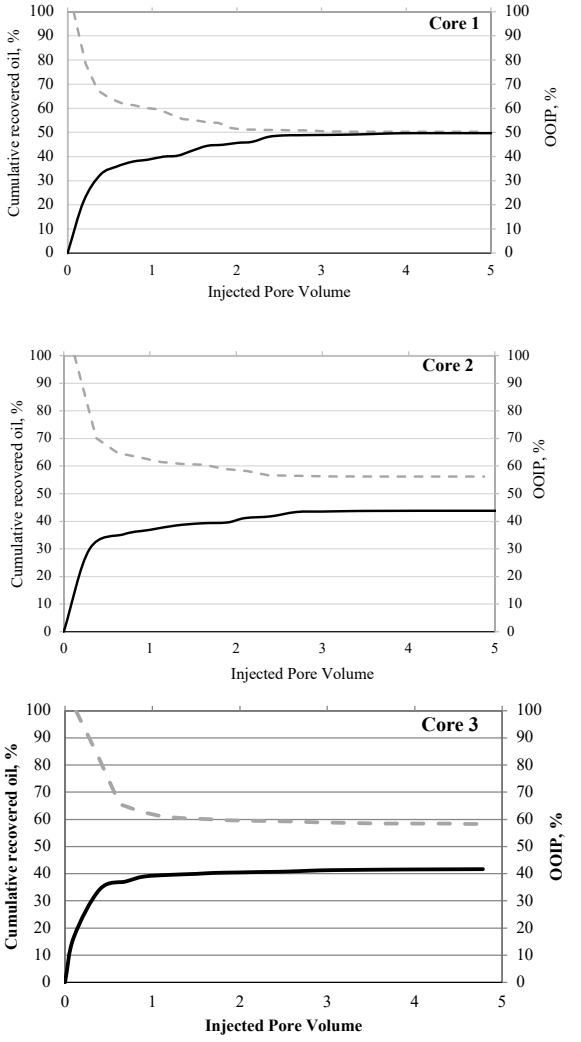

Figure 5. Cumulative oil recovery (solid black line) and oil desaturation (dotted gray line) by water flooding through Berea cores.

this reason, this emulsion was employed in the tests with rock nuclei.

3.2 Emulsion flooding in Berea cores

The injection of brine into the Berea core during the secondary recovery stage occurred as it usually does, from the inlet to the outlet. The data corresponding to the rock properties and oil production during the injection of brine (R_w) are shown in Table 2. Normally water penetrates the smallest pores while oil accumulates in the biggest ones and for this reason, when either water or brine are injected, the oil production rate is higher for the higher permeability porous media, e.g. when 0.4 PV of brine was injected, the recovery percentage of oil in the cores happened as follows: core 1 (32.58 %) ≤ core 2 (32.6 %) < core 3 (34.33 %) (Figure 5). However, as time passes by, the injected water flows through the core, showing the preferential path (in cores with higher permeability, this process takes place faster), leaving part of the water-unswept oil behind. At additional recovery stages, a point is reached at which there is no point in injecting a higher amount of displacing fluid and in the case of the present work, from the injection of 2.5 PVs of brine, the cumulative oil recovery trend remained almost static, and the oil production was practically zero. The rate of oil displaced by brine during the secondary recovery process was slightly higher in the cores with lower permeability: core 3 (45.91 mD) < core 2 (32.77 mD) < core 3 (11.58 mD), which corresponds to 41.68 % < 43.80 % < 49.71 %, leaving around 50 % of residual oil in the core.

After the secondary recovery, the injection of a slug equivalent to 0.1 PV of emulsion aqueous solution was done, which was diluted with distilled water before being used until obtaining 1 wt. % of the dispersed oil phase, through the core face opposite to the brine injection face. Immediately, the injection of brine was resumed. The data corresponding to the oil production during the emulsion flooding are shown in Table 2. By injecting the emulsion and resuming that of brine, it was observed that the oil production occurred sooner in the core with higher permeability: core 1 with 12 mD (1.5 PV of injected brine) < core 2 with 33 mD (1.1 PV of injected brine) ≤ core 3 with 46 mD (0.9 PV of injected brine). After injecting around 2.0-2.2 PV of brine, the cumulative oil recovery reached a maximum for cores 2 and 3 and in order to reach the asymptote of the oil cumulative production curve in the least permeable core (core 1), it was necessary to inject around 3.6 PV of brine (Figure 6). By counting the oil cumulative production at the end of the test, when the recovery of additional oil stopped, the percentage was slightly higher in the test performed with the higher permeability core: core 1 (9.55 %) ≤ core 2 (10.66 %) < core 3 (13.35 %). Even by analyzing the additional oil recovery data based on residual oil that was left in the core after the secondary recovery and carrying out the computations

Table 3. Properties of the Berea core and oil recovery measured with the tomography test.

Core	L [m]	D [m]	k_0 [mD]	φ_0 [%]	Initial oil saturation [%]	Cumulative oil recovery [%]			
						Water flooding, R_w	Emulsion flooding, R_e	Total	Residual oil recovery, R_r
4	0.1000	0.0508	41.62	18.38	77.73	71.28	9.62	80.90	33

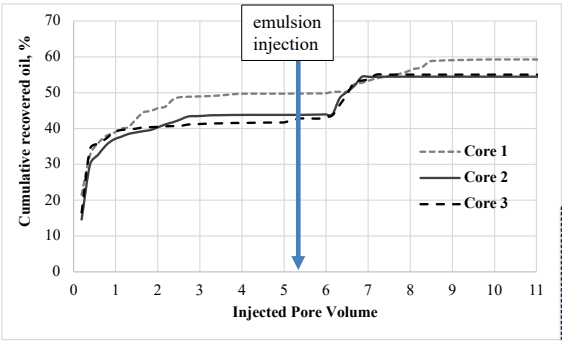

Figure 6. Cumulative oil recovery by water and emulsion flooding through Berea cores.

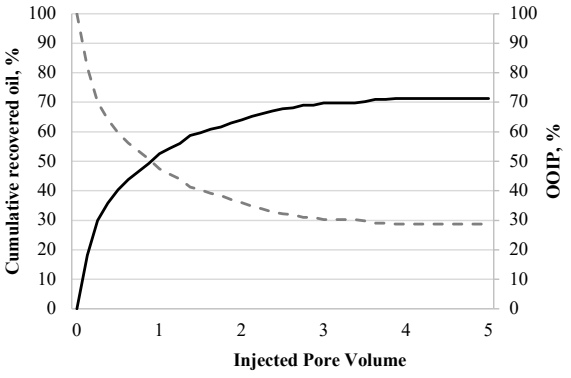

Figure 7. Cumulative oil recovery (solid black line) and oil desaturation (dotted gray line) by water flooding through Berea core 4 during the tomography test.

according to the formula $100 * R_e/(100 - R_w)$, slightly enhanced recovery in the core with higher permeability was confirmed: core 1 (19 %) = core 2 (19 %) < core 3 (23 %). Despite the final percentages of additional recovery for the three cores are very similar, the production rate was more attractive with core 3 (45.91 mD) than with core 1 (11.58 mD).

3.3 Tomography of the core emulsion flooding

The injection of brine into the Berea core during the water flooding stage occurred like in the previous tests: from the inlet to the outlet, recovering up to 71 % of original oil in the core (Table 3), which was higher than the one obtained with previous experiments (Table 2), because the injection rate (5 cm^3/h) was lower than the one used in previous experiments (10 cm^3/h); for this reason, the penetration of displacing

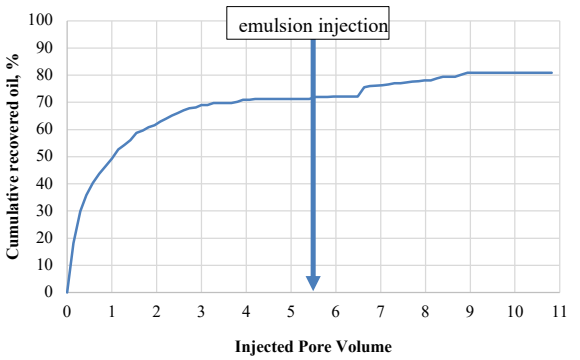

Figure 8. Cumulative oil recovery by water and emulsion flooding through Berea core during the tomography test.

fluid was more uniform and it can be seen that in the cumulative oil recovery and oil desaturation curves in Figure 7 do not display abrupt falls and the trend remained almost static from the injection of 4 PV. The top oil production by water flooding took place during the first process moments. Afterward, the displacing fluid formed preferential channels and remaining oil was in isolated zones, which makes impossible to recover all the oil saturating the core.

After the secondary recovery, an emulsion slug equivalent to 10 % of the PV was injected from the core inlet face, which was the same as that of brine. It is worth emphasizing that during this step, oil recovery was not observed. Once the chemical product was inserted, the brine was injected again at 5 cm^3/h. The flow displacement occurred from the inlet to the outlet of the core, recovering 9.62 % of original core oil.

As the core desaturates, oil is produced. After injecting 3.53 PV, the trend continued practically constant and neither more oil was produced nor the core kept desaturating (Figure 8), for there is a point at which residual oil inside the pores cannot move. Then, it can be inferred that the injection of the chemical compound was successful, with 33 % of residual oil recovery from the core, because the emulsion plugged the preferential channels through which the fluid (brine) flowed initially. Having the preferential channels plugged, brine flows through new paths represented by porous spaces that had not been previously flooded, which enables brine to push oil volumes that had not been swept by water at an earlier stage. The recovery mechanism turns around the increasing swept volume without affecting the interfacial tension change; for this reason, not all the residual oil that remained after the secondary recovery

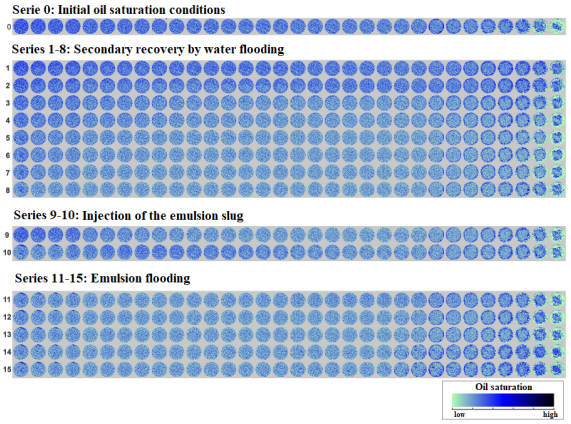

Figure 9. Plate with tomography images: the 0 series represents the initial oil saturation conditions and S_{wr}; the 1-8 series corresponds to the secondary recovery by water flooding; the 9-10 series refers to the density change effect provoked by the transition of the injection of the emulsion slug; and the 11-15 series shows the saturation transition of residual oil during the tertiary recovery process by emulsion flooding.

was recovered. Notwithstanding, with just 10 % of the injected PV of the emulsion with 1 wt.% of the dispersed oil phase, the oil recovery increased in 9.62 % of the original oil, which confirmed that this method is a good alternative for the EOR technique.

During the additional recovery process, two series of X-ray tomography images were taken (Figure 9): under dry conditions and saturated with water at 100 %. In this way, the rock porosity distribution and oil saturation in the core during the initial stages, water and emulsion flooding, of the recovery experiment were determined.

The tomography images revealed how the oil saturation changed in the core during the oil recovery process. The oil saturation diminished drastically at the end of the secondary recovery stage (8 series). By injecting an emulsion slug of 0.1 PV, and resuming the injection of water, it was possible to see that oil was pushed by the displacing fluid toward the core outlet, which is illustrated in the images corresponding to the 14-15 series.

The oil recovery process with an emulsion slug of 0.1 PV was more efficient for the tomography test, which simulated "two wells" (Table 3), than the tests simulating "a single well" (Table 2). This happened, based on the tomography images, because after the emulsion flooding (series 13 and 14) there was more intensive oil saturation at the core outlet (right side) than at the inlet (left side).

Based on the experiment data from tomography test (Figure 8) performed to study the displacement of residual oil by the emulsion, the theoretical analysis for multiphase flow in porous media was carried out by fitting the oil production curves in the tomography experiment using STARS^{TM} by CMG; based on this

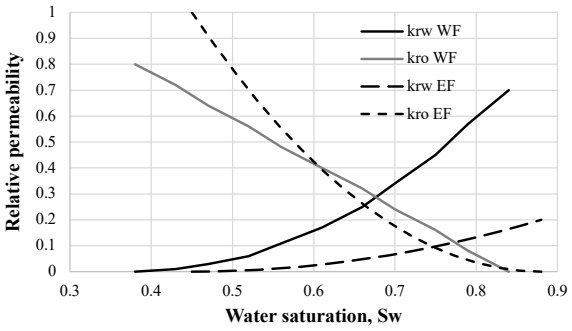

Figure 10. Relative permeabilities of water (krw) and oil (kro) for water flooding (WF) and emulsion flooding (EF).

fitting process, the relative permeabilities for the water and oil phases were calculated (Figure 10). The critical water saturation for WF was 0.38 and for EF was 0.45, the residual oil saturation decreased from 0.15 for WF to 0.12 for EF. The end points for water permeability curve decreased from 0.7 to 0.2, while for oil permeability curve increased from 0.8 to 1, meaning that oil mobility increased as the water flow progressed more slowly. The relative permeability curves indicate that after emulsion flooding, the rock became more water wettable, which was confirmed by the X-ray tomography images (Figure 9). The images corresponding to series 13 and 14 show that at the end of the test, 70 % of the core was saturated mainly by water, whereas oil was displaced to the core exit, where residual oil saturation (according to the images) was higher, confirmed the increase in oil mobility in the core.

The recovery percentage achieved with the emulsion injection was due to soft plugging of the pore throats, where the emulsion remained trapped, thus changing the pattern of the water preferential channels; with further penetration, water reached zones that had not been previously touched during the water flooding operation as secondary recovery technique.

Conclusion

- Based on the carried out experiments, it was determined that at a stirring rate equal to 16,000 rpm, stirring time of 8 min, and 3 % of the concentration of the emulsifier Igepal CO 720, with HLB equal to 16, it was possible to form O/W type emulsions stable for 1 month, where 70 % corresponded to the dispersed oil phase with an average size of the dispersed droplets equal to 0.9 μm.

- By injecting 0.1 PV of emulsion slug of diluted O/W emulsion at 1 wt.% of the dispersed

oil phase through sandstone cores, after the secondary recovery process, from the core face opposite to the brine injection face, imitating "a single oil well", the additional oil recovery was promoted, with higher final percentages (23 %) and oil recovery rate for the core with higher permeability (46 mD).

- The tomography test simulating "two wells" showed that the residual oil recovery equivalent to 33 % was attributed to the redistribution of fluids inside the core and to greater sweeping area after the injection of a slug of diluted O/W emulsion, which was caused by the dispersed emulsion drops blocking the preferential channels of water that forced it to penetrate zones that had not been previously flooded.
- The theoretical analysis for multiphase flow in porous media indicates that after emulsion flooding, the oil mobility increased while that of water decreased.

Acknowledgements

Thanks are due to David Iván Ricárdez Frías for his contribution to the experimental development of this work.

Nomenclature

Capillary number	(Nc)
Enhanced oil recovery	(EOR)
Light Obscuration	(LO)
Oil-in-water	(O/W)
Porous volume	(PV)
Single Particle Optical Sensing	(SPOS)

References

Baldygin, A., Nobes, D. S., & Mitra, S. K. (2014). Water-alternate-emulsion (WAE): A new technique for enhanced oil recovery. *Journal of Petroleum Science and Engineering*, *121*, 167-173. https://doi.org/10.1016/j.petrol.2014.06.021

Cardenas, R. L., Harnsberger, B. G., & Jr, J. M. (1981). *Emulsion oil recovery process usable in high temperature, high salinity formations* (United States Patent US4270607A). https://patents.google.com/patent/US4270607A/en?q=Emulsion+oil+recovery+process+usable+in+high+temperature%2c+high+salinity+formations&oq=Emulsion+oil+recovery+process+usable+in+high+temperature%2c+high+salinity+formations

Castillo-Campos, E., Mugica-Álvarez, V., Roldán-Carillo, T. G., Olguín-Lora, P., Castorena-Cortés, G. T., (2021). Modification of wettability and reduction of interfacial tension mechanisms involved in the release and enhanced biodegradation of heavy oil by a biosurfactant. *Revista Mexicana de Ingeniería Química*, *20*(3), 1-15. https://doi.org/10.24275/rmiq/IA2427

de Castro Dantas, T. N., de Souza, T. T. C., Dantas Neto, A. A., Moura, M. C. P. de A., & de Barros Neto, E. L. (2017). Experimental Study of Nanofluids Applied in EOR Processes. *Journal of Surfactants and Detergents*, *20*(5), 1095-1104. https://doi.org/10.1007/s11743-017-1992-2

de Farias, M. L., de Souza, A. L., da Silveira Carvalho, M. ., Hirasaki, G. ., & Miller, C. . (2012). *A Comparative Study of Emulsion Flooding and other IOR Methods for Heavy Oil*. SPE-152290-MS. https://doi.org/10.2118/152290-MS

Demikhova, I. I., Likhanova, N. V., Hernandez Perez, J. R., Falcon, D. A. L., Olivares-Xometl, O., Moctezuma Berthier, A. E., & Lijanova, I. V. (2016). Emulsion flooding for enhanced oil recovery: Filtration model and numerical simulation. *Journal of Petroleum Science and Engineering*, *143*, 235-244. https://doi.org/10.1016/j.petrol.2016.02.018

Demikhova, I. I., Likhanova, N. V., Moctezuma, A. E., Hernandez Perez, J. R., Olivares-Xometl, O. ., & Lijanova, I. V. (2014). Improved Oil Recovery Potential by Using Emulsion Flooding. *All Days*, SPE-171146-MS. https://doi.org/10.2118/171146-MS

Ding, B., Yu, L., Dong, M., & Gates, I. (2019). Study of conformance control in oil sands by oil-in-water emulsion injection using heterogeneous parallel-sandpack models. *Fuel*, *244*, 335-351. https://doi.org/10.1016/j.fuel.2019.02.021

Du, X., Liu, T., Xi, C., Wang, B., Qi, Z., Zhou, Y., Xu, J., Lin, L., Istratescu, G., Babadagli, T., & Li, H. A. (2023). Can hot water injection with chemical additives be an alternative to steam injection: Static and dynamic experimental evidence. *Fuel*, *331*, 125751. https://doi.org/10.1016/j.fuel.2022.125751

Engelke, B., Carvalho, M. S., & Alvarado, V. (2013). Conceptual Darcy-Scale Model of Oil

Displacement with Macroemulsion. *Energy & Fuels*, *27*(4), 1967-1973. https://doi.org/10.1021/ef301429v

Ge, J., Sun, X., Liu, R., Wang, Z., & Wang, L. (2020). Emulsion Acid Diversion Agents for Oil Wells Containing Bottom Water with High Temperature and High Salinity. *ACS Omega*, *5*(45), 29609-29617. https://doi.org/10.1021/acsomega.0c04767

Goswami, R., Chaturvedi, K. R., Kumar, R. S., Chon, B. H., & Sharma, T. (2018). Effect of ionic strength on crude emulsification and EOR potential of micellar flood for oil recovery applications in high saline environment. *Journal of Petroleum Science and Engineering*, *170*, 49-61. https://doi.org/10.1016/j.petrol.2018.06.040

Guillen, V. R., Romero, M. I., Carvalho, M. D. S., & Alvarado, V. (2012). Capillary-driven mobility control in macro emulsion flow in porous media. *International Journal of Multiphase Flow*, *43*, 62-65. https://doi.org/10.1016/j.ijmultiphaseflow.2012.03.001

Hamidi, H., Mohammadian, E., Asadullah, M., Azdarpour, A., & Rafati, R. (2015). Effect of ultrasound radiation duration on emulsification and demulsification of paraffin oil and surfactant solution/brine using Hele-shaw models. *Ultrasonics Sonochemistry*, *26*, 428-436. https://doi.org/10.1016/j.ultsonch.2015.01.009

Hernandez-Perez, J., Likhanova, N., Lopez-Falcon, D., Olivares-Xometl, O., Munoz-Salazar, L., & Trejo-Zarraga, F. (2022). Efficient use of oil in water macroemulsions as enhanced oil recovery agents. *Petroleum Science and Technology*, *40*(2), 201-216. https://doi.org/10.1080/10916466.2021.1992422

Hou, X., & Sheng, J. J. (2023). Properties, preparation, stability of nanoemulsions, their improving oil recovery mechanisms, and challenges for oil field applications—A critical review. *Geoenergy Science and Engineering*, *221*, 211360. https://doi.org/10.1016/j.geoen.2022.211360

Jalilian, M., Tabzar, A., Ghasemi, V., Mohammadzadeh, O., Pourafshary, P., Rezaei, N., & Zendehboudi, S. (2019). An experimental investigation of nanoemulsion enhanced oil recovery: Use of unconsolidated porous systems. *Fuel*, *251*, 754-762. https://doi.org/10.1016/j.fuel.2019.02.122

Jiang, K., Xiong, C., Ding, B., Geng, X., Liu, W., Chen, W., Huang, T., Xu, H., Xu, Q., & Liang, B. (2023). Nanomaterials in EOR: A Review and Future Perspectives in Unconventional Reservoirs. *Energy & Fuels*, *37*(14), 10045-10060. https://doi.org/10.1021/acs.energyfuels.3c01146

Karambeigi, M. S., Abbassi, R., Roayaei, E., & Emadi, M. A. (2015). Emulsion flooding for enhanced oil recovery: Interactive optimization of phase behavior, microvisual and core-flood experiments. *Journal of Industrial and Engineering Chemistry*, *29*, 382-391. https://doi.org/10.1016/j.jiec.2015.04.019

Kumar, G., Mani, E., & Sangwai, J. S. (2023). Impact of surface-modified silica nanoparticle and surfactant on the stability and rheology of oil-in-water Pickering and surfactant-stabilized emulsions under high-pressure and high-temperature. *Journal of Molecular Liquids*, *379*, 121620. https://doi.org/10.1016/j.molliq.2023.121620

Kumar, N., Pal, N., & Mandal, A. (2021). Nanoemulsion flooding for enhanced oil recovery: Theoretical concepts, numerical simulation and history match. *Journal of Petroleum Science and Engineering*, *202*, 108579. https://doi.org/10.1016/j.petrol.2021.108579

Lakatos, I., Lakatos-Szabó, J., Bódi, T., & Vágó, Á. (2008). *New Alternatives of Water Shutoff Treatments: Application of Water Sensitive Metastable Systems*. SPE-112403-MS. https://doi.org/10.2118/112403-MS

Lakatos, I., Tóth, J., Bauer, K., Lakatos-Szabó, J., Palásthy, Gy., & Wöltje, H. (2003). *Comparative Study of Different Silicone Compounds as Candidates for Restriction of Water Production in Gas Wells*. SPE-80204-MS. https://doi.org/10.2118/80204-MS

Lakatos, I., Tóth, J., Lakatos-Szabó, J., Kosztin, B., Palásthy, Gy., & Wöltje, H. (2002). *Application of Silicone Microemulsion for Restriction of Water Production in Gas Wells*. SPE-78307-MS. https://doi.org/10.2118/78307-MS

Liu, J., Liu, S., Zhong, L., Wang, P., Gao, P., & Guo, Q. (2023). Ultra-low interfacial tension Anionic/Cationic surfactants system with excellent emulsification ability for enhanced oil recovery. *Journal of Molecular Liquids*, *382*, 121989. https://doi.org/10.1016/j.molliq.2023.121989

Liu, Z., Li, Y., Luan, H., Gao, W., Guo, Y., & Chen, Y. (2019). Pore scale and macroscopic visual displacement of oil-in-water emulsions for enhanced oil recovery. *Chemical Engineering Science*, *197*, 404-414. https://doi.org/10.1016/j.ces.2019.01.001

Lu, X., & Wang, M. (2023). Shape and surface property effects on displacement enhancement by nanoparticles. *International Journal of Mechanical Sciences*, *255*, 108471. https://doi.org/10.1016/j.ijmecsci.2023.108471

Mohamed, A. I. A., Hussein, I. A., Sultan, A. S., & Al-Muntasheri, G. A. (2018). Use of organoclay as a stabilizer for water-in-oil emulsions under high-temperature high-salinity conditions. *Journal of Petroleum Science and Engineering*, *160*, 302-312. https://doi.org/10.1016/j.petrol.2017.10.077

Moradi, M., Kazempour, M., French, J. T., & Alvarado, V. (2014). Dynamic flow response of crude oil-in-water emulsion during flow through porous media. *Fuel*, *135*, 38-45. https://doi.org/10.1016/j.fuel.2014.06.025

Narukulla, R., Ojha, U., & Sharma, T. (2020). Effect of NaCl concentration on stability of a polymer–Ag nanocomposite based Pickering emulsion: Validation *via* rheological analysis with varying temperature. *RSC Advances*, *10*(36), 21545-21560. https://doi.org/10.1039/D0RA03199B

O. Olivares-Xometl, N V. Likhanova, I. V. Lijanova, P Arellanes-Lozada, J. Arriola-Morales, & J. López-Rodríguez. (2021). Injection of emulsions into cores packed Ottawa sand and Berea sandstone as a method for enhanced oil recovery. *Revista Mexicana de Ingeniería Química*, *20*(3). https://doi.org/10.24275/rmiq/Ener2394

Ponce F., R. V., Alvarado, V., & Carvalho, M. S. (2017). Water-alternating-macroemulsion reservoir simulation through capillary number-dependent modeling. *Journal of the Brazilian Society of Mechanical Sciences and Engineering*, *39*(10), 4135-4145. https://doi.org/10.1007/s40430-017-0885-7

Santanna, V. C., Silva, A. C. M., Lopes, H. M., & Sampaio Neto, F. A. (2013). Microemulsion flow in porous medium for enhanced oil recovery. *Journal of Petroleum Science and Engineering*, *105*, 116-120. https://doi.org/10.1016/j.petrol.2013.03.015

Schramm, L. L. (2006). *Emulsions, Foams, and Suspensions: Fundamentals and Applications*. Wiley. https://books.google.es/books?id=9JMrTZxPd2MC

ShamsiJazeyi, H., Miller, C. A., Wong, M. S., Tour, J. M., & Verduzco, R. (2014). Polymer-coated nanoparticles for enhanced oil recovery. *Journal of Applied Polymer Science*, *131*(15), n/a-n/a. https://doi.org/10.1002/app.40576

Sharma, T., Kumar, G. S., Chon, B. H., & Sangwai, J. S. (2015). Thermal stability of oil-in-water Pickering emulsion in the presence of nanoparticle, surfactant, and polymer. *Journal of Industrial and Engineering Chemistry*, *22*, 324-334.

Sharma, T., Velmurugan, N., Patel, P., Chon, B. H., & Sangwai, J. S. (2015). Use of Oil-in-water Pickering Emulsion Stabilized by Nanoparticles in Combination With Polymer Flood for Enhanced Oil Recovery. *Petroleum Science and Technology*, *33*(17-18), 1595-1604. https://doi.org/10.1080/10916466.2015.1079534

Shupe, R. D., & Jr, J. M. (1981). *Emulsion oil recovery process usable in high temperature, high salinity formations* (United States Patent US4269271A). https://patents.google.com/patent/US4269271A/en

Wang, X., Wang, F., Taleb, M. A. M., Wen, Z., & Chen, X. (2022). A Review of the Seepage Mechanisms of Heavy Oil Emulsions during Chemical Flooding. *Energies*, *15*(22), 8397. https://doi.org/10.3390/en15228397

Wang, Z., Babadagli, T., & Maeda, N. (2021). Preliminary Screening and Formulation of New Generation Nanoparticles for Stable Pickering Emulsion in Cold and Hot Heavy-Oil Recovery. *SPE Reservoir Evaluation & Engineering*, *24*(01), 66-79. https://doi.org/10.2118/200190-PA

Xu, K., Zhu, P., Colon, T., Huh, C., & Balhoff, M. (2017). A Microfluidic Investigation of the Synergistic Effect of Nanoparticles and Surfactants in Macro-Emulsion-Based Enhanced Oil Recovery. *SPE Journal*, *22*(02), 459-469. https://doi.org/10.2118/179691-PA

Yadali Jamaloei, B., & Kharrat, R. (2010). Analysis of Microscopic Displacement Mechanisms of Dilute Surfactant Flooding in Oil-wet and Water-wet Porous Media. *Transport in Porous Media*, *81*(1), 1-19. https://doi.org/10.1007/s11242-009-9382-5

Yoon, K. Y., Son, H. A., Choi, S. K., Kim, J. W., Sung, W. M., & Kim, H. T. (2016). Core Flooding of Complex Nanoscale Colloidal Dispersions for Enhanced Oil Recovery by in Situ Formation of Stable Oil-in-Water Pickering Emulsions. *Energy & Fuels*, *30*(4), 2628-2635. https://doi.org/10.1021/acs.energyfuels.5b02806

Yousufi, M. M., Elhaj, M. E. M., Moniruzzaman, M., Ayoub, M. A., Nazri, A. B. M., Husin, H. B., & Saaid, I. B. M. (2019). Synthesis and evaluation of Jatropha oil-based emulsified acids for matrix acidizing of carbonate rocks. *Journal of Petroleum Exploration and Production Technology*, *9*(2), 1119-1133. https://doi.org/10.1007/s13202-018-0530-8

Zabar, M. K., Phan, C. M., & Barifcani, A. (2023). Quantifying the spontaneous emulsification of a heavy hydrocarbon with the presence of a strong surfactant. *Colloids and Surfaces A: Physicochemical and Engineering Aspects*, *656*, 130425. https://doi.org/10.1016/j.colsurfa.2022.130425

Zhang, L., Lei, Q., Luo, J., Zeng, M., Wang, L., Huang, D., Wang, X., Mannan, S., Peng, B., & Cheng, Z. (2019). Natural Halloysites-Based Janus Platelet Surfactants for the Formation of Pickering Emulsion and Enhanced Oil Recovery. *Scientific Reports*, *9*(1), 163. https://doi.org/10.1038/s41598-018-36352-w

Zhang, Z., Wang, Y., Ding, M., Mao, D., Chen, M., Han, Y., Liu, Y., & Xue, X. (2023). Effects of viscosification, ultra-low interfacial tension, and emulsification on heavy oil recovery by combination flooding. *Journal of Molecular Liquids*, *380*, 121698. https://doi.org/10.1016/j.molliq.2023.121698

Zhou, Y., Yin, D., Chen, W., Liu, B., & Zhang, X. (2019). A comprehensive review of emulsion and its field application for enhanced oil recovery. *Energy Science & Engineering*, *7*(4), 1046-1058. https://doi.org/10.1002/ese3.354

Zhou, Y., Yin, D., Wang, D., & Gao, X. (2018). Emulsion particle size in porous media and its effect on the displacement efficiency. *Journal of Dispersion Science and Technology*, *39*(10), 1532-1536. https://doi.org/10.1080/01932691.2017.1421082